

Identification of Fused-Ring Alkanoic Acids with Improved Pharmacokinetic Profiles that Act as G Protein-Coupled Receptor 40/Free Fatty Acid Receptor 1 Agonists

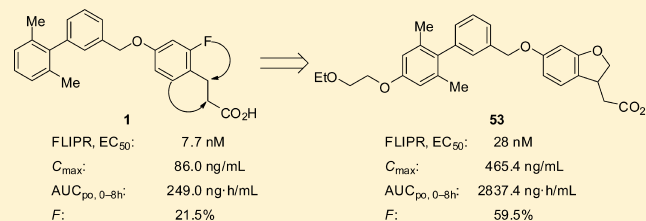
Nobuyuki Negoro,^{*,†} Shinobu Sasaki,[†] Masahiro Ito,[†] Shuji Kitamura,[†] Yoshiyuki Tsujihata,[†] Ryo Ito,[†] Masami Suzuki,[†] Koji Takeuchi,[†] Nobuhiro Suzuki,[‡] Junichi Miyazaki,[‡] Takashi Santou,[†] Tomoyuki Odani,[†] Naoyuki Kanzaki,[†] Miyuki Funami,[‡] Toshimasa Tanaka,[†] Tsuneo Yasuma,[‡] and Yu Momose[†]

[†]Pharmaceutical Research Division, Takeda Pharmaceutical Company Limited, 26-1 Muraoka-Higashi 2-chome, Fujisawa, Kanagawa 251-8555, Japan

[‡]Pharmaceutical Research Division, Takeda Pharmaceutical Company Limited, 17-85 Jusohonmachi 2-chome, Yodogawa-ku, Osaka 532-8666, Japan

S Supporting Information

ABSTRACT: The G protein-coupled receptor 40 (GPR40)/free fatty acid receptor 1 (FFA1) has emerged as an attractive target for a novel insulin secretagogue with glucose dependency. We previously identified phenylpropanoic acid derivative **1** (3-{4-[(2',6'-dimethylbiphenyl-3-yl)methoxy]-2-fluorophenyl}propanoic acid) as a potent and orally available GPR40/FFA1 agonist; however, **1** exhibited high clearance and low oral bioavailability, which was likely due to its susceptibility to β -oxidation at the phenylpropanoic acid moiety. To identify long-acting compounds, we attempted to block the metabolically labile sites at the phenylpropanoic acid moiety by introducing a fused-ring structure. Various fused-ring alkanolic acids with potent GPR40/FFA1 activities and good PK profiles were produced. Further optimizations of the lipophilic portion and the acidic moiety led to the discovery of dihydrobenzofuran derivative **53** ((6-{[4'-(2-ethoxyethoxy)-2',6'-dimethylbiphenyl-3-yl]methoxy}-2,3-dihydro-1-benzofuran-3-yl)acetic acid), which acted as a GPR40/FFA1 agonist with in vivo efficacy during an oral glucose tolerance test (OGTT) in rats with impaired glucose tolerance.



INTRODUCTION

The G protein-coupled receptor 40 (GPR40)/free fatty acid receptor 1 (FFA1), which is preferentially expressed in pancreatic β -cells, was identified as a receptor for medium- to long-chain free fatty acids (FFAs) such as oleic acid and linoleic acid.¹⁻³ The activation promotes the phospholipase C-mediated hydrolysis of phosphatidylinositol 4,5-bisphosphate into diacylglycerol and inositol triphosphate, activating protein kinase C and mobilizing intracellular Ca²⁺ from the endoplasmic reticulum. The elevated intracellular Ca²⁺ concentration resulting from the activation of GPR40/FFA1 by FFAs may amplify glucose-stimulated insulin secretion (GSIS).^{4,5} Because the downregulation of GPR40/FFA1 by small interfering RNA suppressed the augmentation of FFA-induced insulin secretion in mouse insulinoma MIN6 cells,¹ GPR40/FFA1 is thought to be involved in acute insulin secretion by FFAs.

Although FFAs acutely potentiate insulin secretion in response to plasma glucose levels,⁶ chronically elevated FFAs in plasma exhibit pleiotropic effects, including impaired β -cell function and cell death.^{7,8} Additionally, an excess amount of FFAs is an important component in insulin resistance, which

leads to metabolic syndrome, a series of diseases that include type 2 diabetes, obesity, and hyperlipidemia.⁹

Insulin secretagogues such as sulfonylureas and meglitinides are widely used as one of the first-line drugs in type 2 diabetes therapy.¹⁰ Although sulfonylureas have strong insulinotropic potencies, they promote insulin secretion, even with normal plasma glucose levels.¹¹ Thus, these agents can cause hypoglycemia and apoptosis of pancreatic β -cells with long-term therapy (secondary failure).^{12,13} To eliminate these safety concerns, plasma concentrations of these agents must be carefully controlled. Meglitinides are short-acting insulinotropic agents, which do not have as great a potential for hypoglycemia compared to sulfonylureas. Meglitinides must be administered immediately prior to each meal, which makes their use inconvenient for patients, and their effects are limited to the improvement of postprandial hyperglycemia. Because of these factors, agents that promote GSIS have the potential to replace sulfonylureas as a first-line therapy in patients with type 2 diabetes; for example, dipeptidyl peptidase-4 (DPP-4) inhib-

Received: September 29, 2011

Published: January 16, 2012

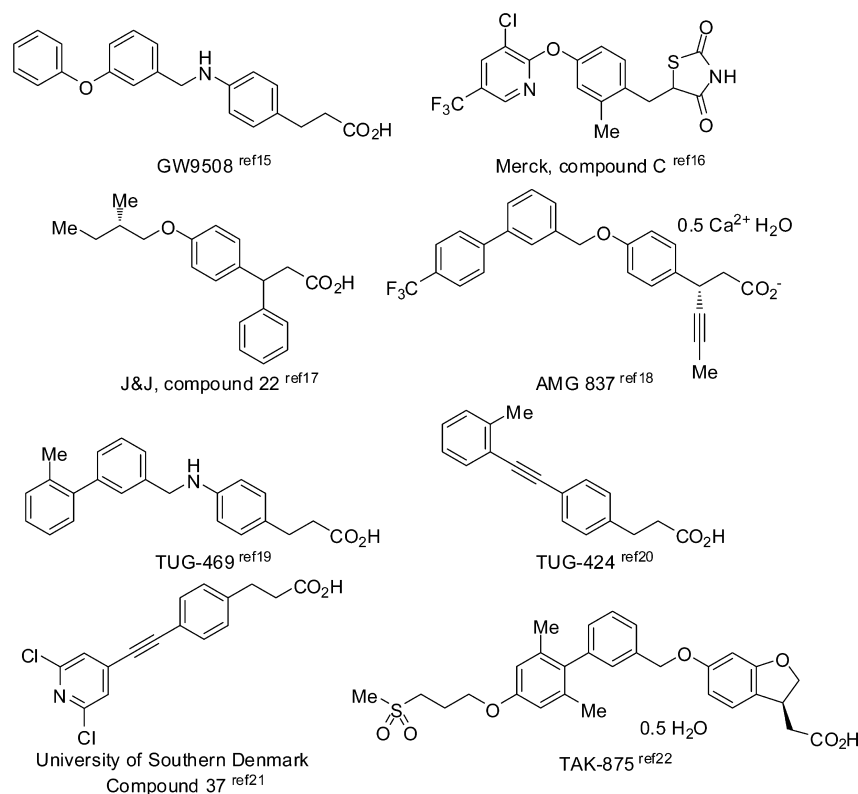


Figure 1. Representative GPR40/FFA1 agonists.

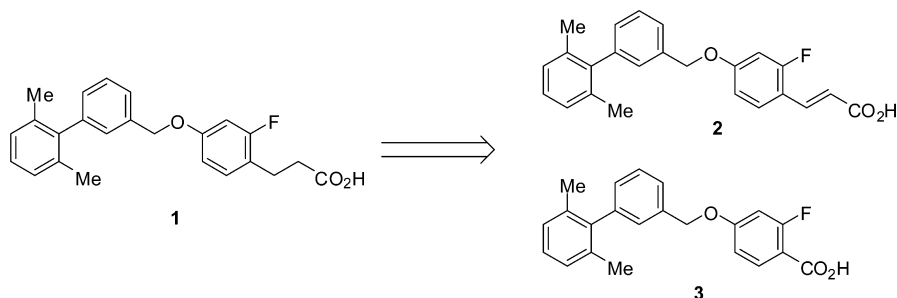


Figure 2. Confirmed structures of metabolites in plasma after oral administration of compound 1 in rats.

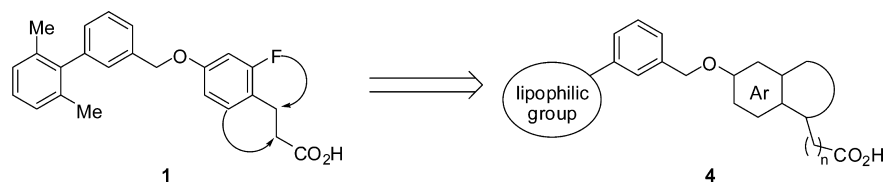


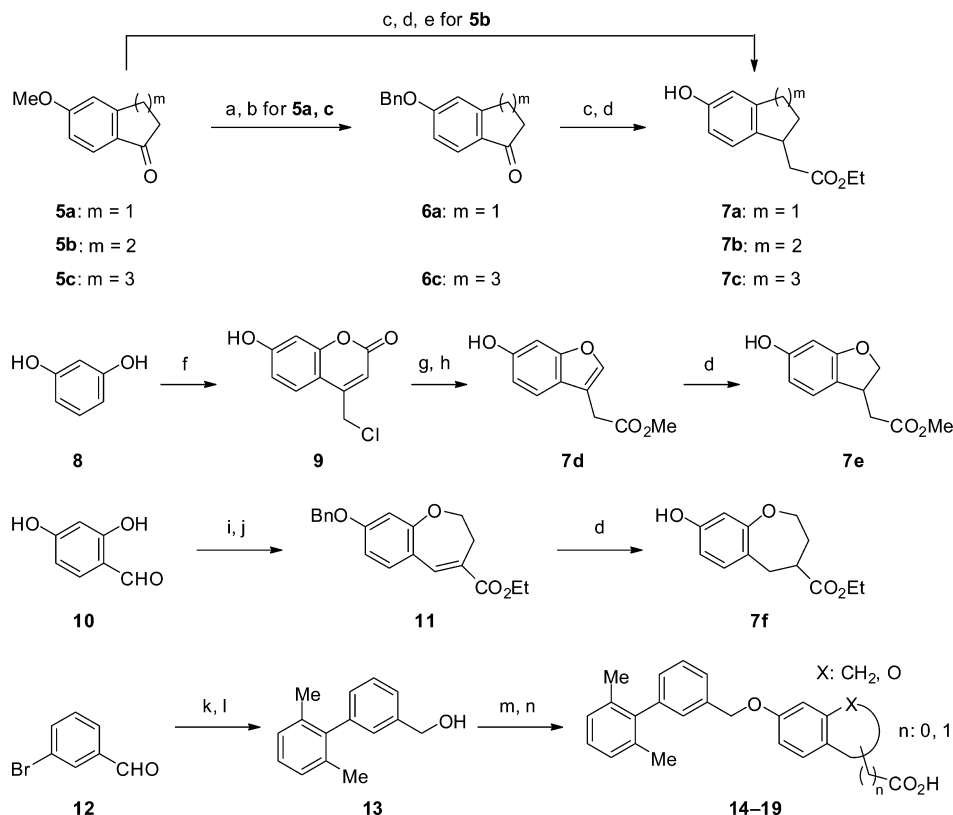
Figure 3. Design of fused-ring alkanolic acids.

itors or peptide-stable analogues of glucagon-like peptide-1 (GLP-1)¹⁴ have got much attention as a new-generation of antidiabetic drugs.

In the development of a novel insulinotropic agent, GPR40/FFA1 is attractive because of a number of reasons. First, GPR40/FFA1 agonists can directly increase Ca^{2+} concentrations in pancreatic β -cells, enabling a robust insulinotropic effect on both postprandial and fasting hyperglycemia. Second, because GPR40/FFA1-mediated insulinotropic actions are glucose-dependent, there may be a low risk of hypoglycemia; thus, we aimed to design a drug with a long duration in plasma. Furthermore, the dominant expression of GPR40/FFA1 in

pancreatic β -cells indicated exclusive efficacy on islets and the reduced side effects derived from GPR40/FFA1 in other tissues.

Figure 1 summarizes a variety of synthetic GPR40/FFA1 agonists such as phenylpropanoic acid and thiazolidinedione derivatives reported by several groups^{14–21} and also represents our clinical candidate TAK-875 under phase 3 development.²² We independently identified a diverse series of GPR40/FFA1 agonists as type 1 using an endogenous ligand-based design (Figure 2).²³ The compound exhibited potent agonist activity and a significant insulinotropic effect in diabetic animal models. In this compound series, introduction of substituents at the

Scheme 1^a

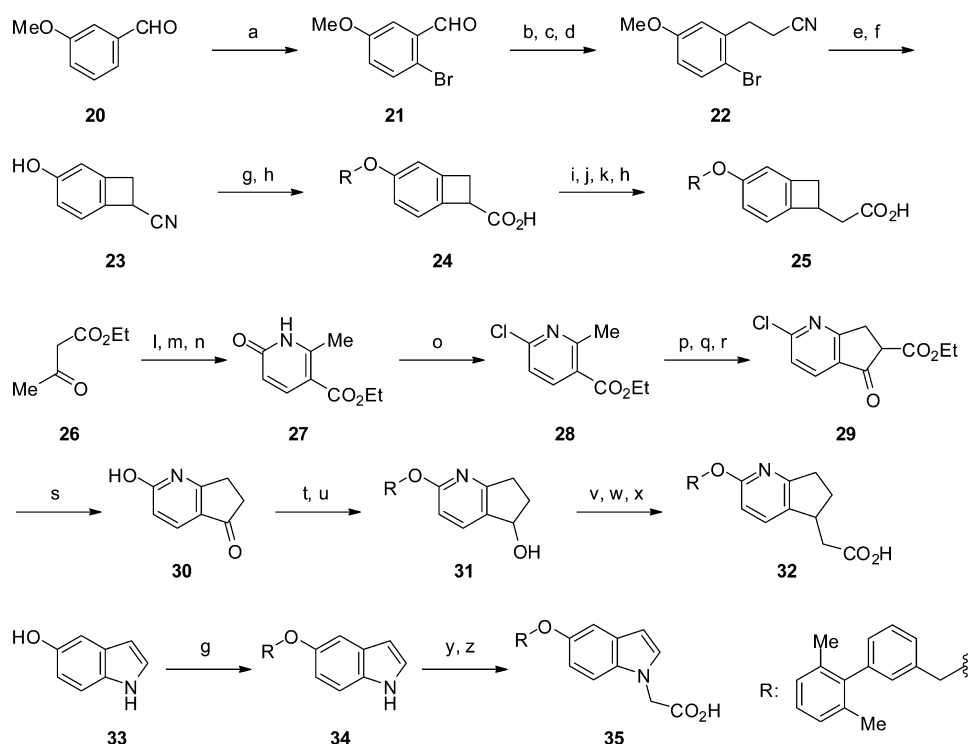
^aReagents and conditions: (a) AlCl₃, toluene, reflux; (b) benzyl bromide, K₂CO₃, acetone, reflux, 91–94% (2 steps); (c) triethyl phosphonoacetate, NaH, toluene, reflux; (d) H₂ (balloon pressure), 10% Pd/C, EtOH or MeOH, rt, 54–89% (2 steps), 76–100% for 7e,f; (e) AlCl₃, 1-dodecanethiol, toluene, rt, 98%; (f) ethyl 4-chloroacetate, H₂SO₄, rt, 84%; (g) 1 M NaOH aq, reflux, 83%; (h) H₂SO₄, MeOH, reflux, 70%; (i) benzyl chloride, KF, CH₃CN, reflux, 43%; (j) ethyl 4-bromobutyrate, Cs₂CO₃, DMF, 80 °C, 41%; (k) 2,6-dimethylphenylboronic acid, Pd(PPh₃)₄, 1 M Na₂CO₃ aq, EtOH, toluene, reflux, 97%; (l) NaBH₄, DME, THF, 0 °C, 83%; (m) 7a–f, ADDP, P(*n*-Bu)₃, toluene, rt, 23–96%; (n) 2 M NaOH aq, MeOH or EtOH, THF, rt, 53–80%.

ortho-position of the phenylpropanoic acid moiety might improve susceptibility to β -oxidation and the resulting *ortho*-fluoro derivative **1** showed moderate bioavailability. However, the β -oxidation was not suppressed completely and the β -oxidation metabolites of **1** such as cinnamic acid **2** and benzoic acid **3** were actually observed in rat plasma (Figure 2). The PK profile of **1** was not yet sufficient, especially regarding the duration in plasma. Therefore, to develop a drug administered once daily for the convenience for patients, we thought that it would be needed to further improve the duration in plasma. With a view to improving metabolic stability of **1** against β -oxidation again, we developed a design strategy to block the α - or β -position of the propanoic acid moiety by constructing a fused-ring structure between the *ortho*-position of the phenyl ring and either site of the propanoic acid (α - or β -position) (Figure 3).

Herein, we describe the identification of fused-ring alkanoids as novel GPR40/FFA1 agonists with low clearance and high plasma exposure in rats consistent with the blockade of β -oxidation. Additionally, we evaluated the species differences between humans and rats in the binding affinity using a GPR40/FFA1 homology model and determined the *in vivo* efficacy by conducting an oral glucose tolerance test (OGTT) in female Wistar fatty rats.

CHEMISTRY

The syntheses of the fused-ring alkanoids **14–19** are detailed in Scheme 1.²² The preparation of the 5-hydroxyindane intermediate **7a** began with the conversion of 5-methoxy-1-indanone (**5a**) to 5-benzyloxy-1-indanone (**6a**). Horner–Wadsworth–Emmons olefination of **6a**, which was followed by catalytic hydrogenation, afforded **7a**. The 6-membered analogue **7b** was synthesized from 6-methoxy-1-tetralone (**5b**) without exchanging the protecting group as shown in the synthesis of **7a**. Incorporation of the acetic acid moiety, followed by deprotection of the methoxy group using Node's method,²⁴ produced **7b**. Similar conditions to **7a** provided the seven-membered analogue **7c** from 2-methoxy-6,7,8,9-tetrahydro-5H-benzo[7]annulen-5-one (**5c**), easily prepared from 3-methoxybenzaldehyde in a four-step sequence. The synthesis of the benzofuran intermediate **7d** began with resorcinol (**8**), followed by Pechmann reaction²⁵ to afford 7-hydroxy-4-chloromethylcoumarin (**9**). Treatment of **9** with an aqueous base triggered the ring-opening and recyclization to form the benzofuran ring,²⁶ followed by esterification to yield the desired product **7d**. Hydrogenation of **7d** resulted in the dihydrobenzofuran intermediate **7e**. The synthesis of 8-hydroxy-tetrahydrobenzoxepine **7f** commenced with the monobenylation of 2,4-dihydroxybenzaldehyde (**10**), which was followed by alkylation with ethyl 4-bromobutyrate and simultaneous cyclization to yield **11**. The catalytic hydrogenation of the

Scheme 2^a

^aReagents and conditions: (a) bromine, AcOH, rt, 88%; (b) cyanoacetic acid, NH_4OAc , pyridine, toluene, reflux, 80%; (c) NaBH_4 , MeOH, satd NaHCO_3 aq, rt, 98%; (d) DMA, 180 °C, 88%; (e) NaNH_2 , NH_3 aq, -33 °C, 48%; (f) AlCl_3 , 1-dodecyl methyl sulfide, toluene, 0 °C, 79%; (g) **13**, ADDP, $P(n\text{-Bu})_3$, toluene or THF, rt, 62–90%; (h) KOH, EtOH, H_2O , rt to reflux, 82–99%; (i) LiAlH_4 , THF, rt, 88%; (j) *p*-TsCl, pyridine, rt, 89%; (k) NaCN, DMSO, rt, 90%; (l) silica gel, NH_3 aq, rt, 67%; (m) methyl propiolate, toluene, reflux; (n) heat, DMF, reflux, 34% (2 steps); (o) POCl_3 , 120 °C, 89%; (p) NBS, AIBN, CCl_4 , reflux, 63%; (q) diethyl malonate, NaH, toluene, rt, 74%; (r) NaH, toluene, reflux, 99%; (s) H_3PO_4 , 185 °C, 85%; (t) **13**, MsCl, Et_3N , THF then **30**, K_2CO_3 , DMF, 70 °C; (u) NaBH_4 , MeOH, THF, 0 °C, 6% (2 steps); (v) SOCl_2 , pyridine, toluene, rt; (w) diethyl malonate, NaH, THF, rt, 53% (2 steps); (x) 2 M NaOH aq, EtOH, THF, 0 °C then toluene, reflux, 38%; (y) ethyl bromoacetate, NaH, THF, DMF, 4 °C to rt, 83%; (z) KOH aq, EtOH, THF, rt, 76%.

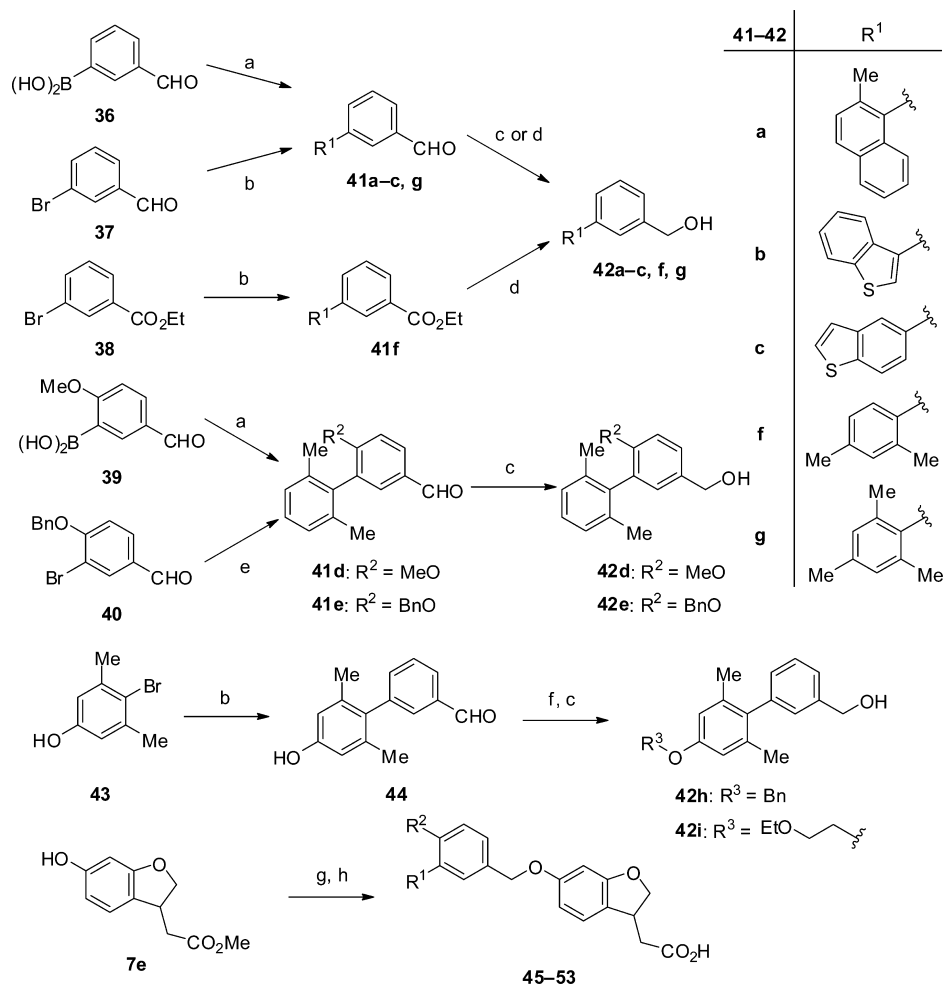
olefin furnished debenzylated product **7f**. The left-hand biphenylmethanol **13** was prepared by Suzuki coupling and subsequent reduction with sodium borohydride. Condensation of **13** with phenols **7a–f** by Mitsunobu reaction, followed by hydrolysis, afforded the desired carboxylic acids **14–19**.

Scheme 2 describes the synthesis of other fused-ring analogues (**25**, **32**, and **35**). Construction of the benzocyclobutene backbone was achieved using a known method.²⁷ The propanenitrile intermediate **22**, prepared from 3-methoxybenzaldehyde (**20**) in a four-step sequence, was treated with sodium amide in liquid ammonia, followed by demethylation with dodecyl methyl sulfide²⁸ to afford **23**. Introduction of the biphenyl region into **23** and subsequently a one-carbon homologation sequence provided the desired benzocyclobuteneacetic acid **25**. The synthesis of dihydrocyclopenta[*b*]-pyridine derivative **32** was accomplished through multistep reactions. The pyridone intermediate **27** was prepared in a three-step sequence using a reported procedure,^{29,30} and it was then treated with phosphorus oxychloride to elaborate chloropyridine **28**. After the benzylic bromination of **28**, the insertion of a malonate unit and the subsequent cyclization with a base afforded the ketoester **29**, which was decarboxylated by heating to give hydroxypyridine **30**. Next, introduction of a biphenyl region to **30** and the subsequent reduction of the carbonyl group produced the alcohol **31**. Subsequent chlorination of **31** with thionyl chloride, alkylation of the resulting chloride with malonate anion, basic hydrolysis, and

finally the following thermal decarboxylation afforded the target compound **32**. The synthesis of the indole derivative **35** was accomplished via attachment of the lipophilic region, insertion of the acetate moiety, and basic hydrolysis.

Next, we fixed (2,3-dihydro-1-benzofuran-3-yl)acetic acid as the acidic region and modified the lipophilic region (Scheme 3). The alcohol intermediates **42a–g** were prepared by Suzuki coupling between the appropriate bromide and boronic acid, followed by the reduction of the ester group or the formyl group. The synthesis of the 4'-alkoxybiphenyl intermediates **42h–i** were obtained via alkylation of the 4'-hydroxybiphenyl intermediate **44**. Condensation of the obtained alcohols **42a–i** with the dihydrobenzofuran intermediate **7e**, followed by basic hydrolysis, afforded the desired carboxylic acids **45–53**.

Next, we again conducted the modification of the acid region with fixing the lipophilic side-chain as the {4'-(2-ethoxyethoxy)-2',6'-dimethylbiphenyl-3-yl}methyl group (Scheme 4). The synthesis of the indan-2-carboxylate intermediate **56a** or the tetrahydronaphthalene-2-carboxylate intermediate **56c** began with the insertion of an ethoxycarbonyl group into the 6-methoxy-1-indanone (**54**) or 6-methoxy-1-tetralone (**57**), respectively. Reductive decarbonylation with TFA/triethylsilane, followed by demethylation, afforded the desired compounds **56a** and **56c**. The synthesis of the isobenzofuran intermediate **56e** was completed in a five-step sequence. Sandmeyer hydroxylation of 5-aminophthalide (**59**) and benzylation of the consequent hydroxy group gave the

Scheme 3^a

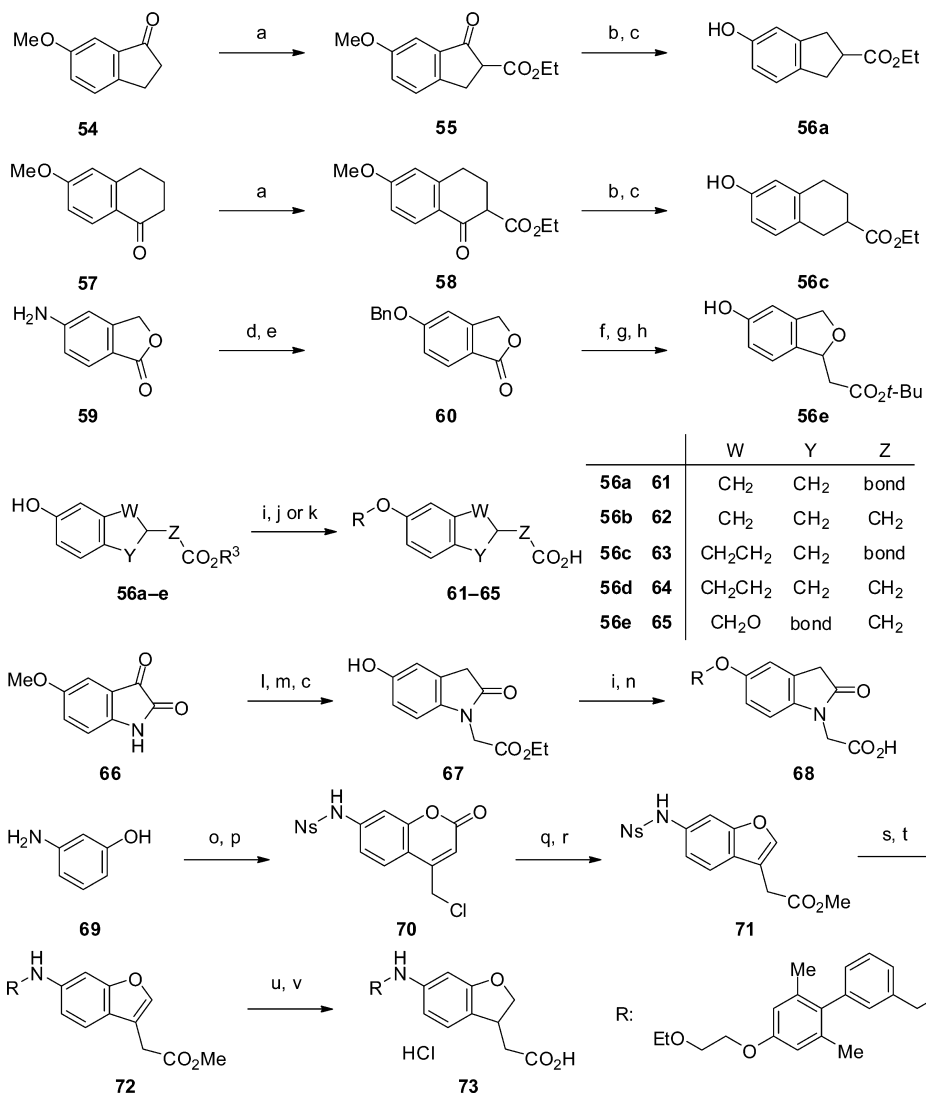
^aReagents and conditions: (a) ArBr, Pd(PPh₃)₄, Cs₂CO₃ or Na₂CO₃, EtOH, toluene, H₂O, 70 °C, 65–94%; (b) ArB(OH)₂, Pd(PPh₃)₄, Cs₂CO₃, EtOH, toluene, 70–80 °C, 76%–quant; (c) NaBH₄, EtOH or DME–THF or MeOH–THF, 0 °C, 70–99%; (d) LiAlH₄, THF, 0 °C to rt, 95–96%; (e) 2,6-dimethylphenylboronic acid, Pd₂(dba)₃, SPhos, K₃PO₄, toluene, H₂O, 100 °C, quant; (f) R³-X, K₂CO₃, (KI), DMF, 70 °C, 89–92%; (g) 42, ADDP, P(*n*-Bu)₃, toluene, rt, 50–93%; (h) 2 M NaOH aq, MeOH, THF, rt, 55–92%.

benzyloxy compound **60**. Treatment with an organolithium reagent that was generated from *tert*-butyl acetate and the subsequent deoxygenation with TFA/triethylsilane, followed by debenylation, produced the desired intermediate **56e**. The target carboxylic acids **61–65** were obtained under the similar conditions described above. The synthesis of the oxyindolyl-acetic acid **68** was initiated with 5-methoxyisatin (**66**). After attachment of the acetate group, the obtained compound was subjected to decarbonylation under hydrogenation conditions in acidic solvent to afford the hydrolyzed oxyindole derivative, which was reesterified and subsequently demethylated to result in the phenol intermediate **67**. Condensation of the lipophilic portion, followed by hydrolysis under acidic condition, produced the desired compound **68**. The 6-aminodihydrobenzofuran derivative **73** was synthesized from 3-aminophenol (**69**) utilizing the 2-nitrobenzenesulfonyl (Ns) group.³¹ After introduction of a Ns group, a similar reaction sequence that was used for the synthesis of **7d** afforded the benzofuran **71**, which was alkylated using Mitsunobu reaction, followed by denosylation with mercaptoacetic acid to give **72**. Finally, the resultant benzofuran **72** was reduced under catalytic hydrogenation conditions, followed by ester hydrolysis to give the desired compound **73** as a hydrochloride salt.

RESULTS AND DISCUSSION

Agonist activities of the synthesized compounds were measured with a fluorometric imaging plate reader (FLIPR) assay in Chinese hamster ovary (CHO) cells expressing human GPR40/FFA1 in the presence of 0.1% bovine serum albumin (BSA). Binding affinities for human and rat receptors were also measured using the membrane fraction of stably expressing GPR40/FFA1 in the presence of 0.2% BSA.²²

First, we examined whether various fused-ring alkanolic acid derivatives, which were designed to suppress β -oxidation, retained potent GPR40/FFA1 activity (Table 1). Nonaromatic four- to six-membered ring fused-benzene derivatives, such as **14**, **15**, and **25**, showed agonist activities comparable to the phenylpropanoic acid **1**, whereas the seven-membered ring acetic acid **16** displayed decreased agonist activity. Interestingly, moving the attachment site from the β -position to the α -position of the propanoic acid moiety, as with 2,3,4,5-tetrahydro-1-benzoxepine-4-carboxylic acid **19**, recovered the agonist activity. Thus, proper placement of the carboxylic group and the phenyl ring may be important for the GPR40/FFA1 agonist activity, regardless of the size of the fused-ring or the construction of a fused-structure at either the α - or β -position

Scheme 4^a

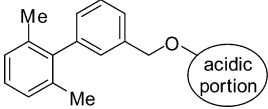
^aReagents and conditions: (a) diethyl carbonate, NaH, toluene, rt to 120 °C, 51–70%; (b) triethylsilane, TFA, rt; (c) AlCl₃, 1-octanethiol, CH₂Cl₂, 0 °C, 32–67% (2 steps), 81% for 67-step 3; (d) H₂SO₄, sodium nitrite, H₂O, 0 °C to reflux; (e) benzyl bromide, K₂CO₃, DMF, 60 °C, 21% (2 steps); (f) *tert*-butyl acetate, lithium diisopropylamide, THF, –78 °C, (g) triethylsilane, TFA, CH₂Cl₂, rt, 16% (2 steps); (h) H₂, Pd/C, EtOH, rt, 86%; (i) 42i, ADDP, (*n*-Bu)₃P, toluene, rt, 22–85%; (j) 1 or 2 M NaOH aq, MeOH or EtOH, THF, rt, 57–91%; (k) TFA, toluene, rt, 72%; (l) ethyl bromoacetate, NaH, DMF, 0 °C to rt, 78%; (m) H₂ (balloon pressure), 10% Pd/C, 70% perchloric acid, AcOH, 50 °C, then SOCl₂, EtOH, rt, 36%; (n) 60% HClO₄, AcOH, 50 °C, 18%; (o) 2-nitrobenzenesulfonyl chloride, pyridine, rt, 77%; (p) ethyl 4-chloroacetate, H₂SO₄, rt, 51%; (q) 1 M NaOH aq, rt, quant; (r) SOCl₂, MeOH, rt, 62%; (s) 42i, DEAD, PPh₃, toluene, rt; (t) mercaptoacetic acid, LiOH·H₂O, DMF, rt 76% (2 steps); (u) H₂ (balloon pressure), 10% Pd/C, EtOH, rt, 66%; (v) 2 M NaOH aq, EtOH, THF, rt, then 4 M HCl/AcOEt, Et₂O, rt, 85%.

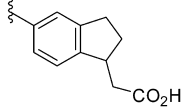
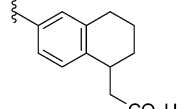
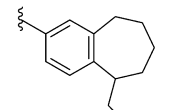
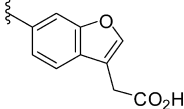
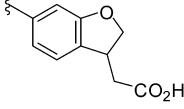
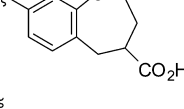
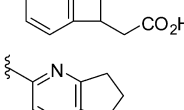
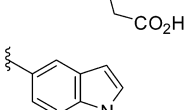
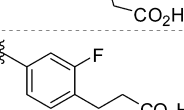
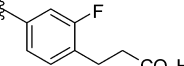
of the propanoic acid moiety. Replacement of the methylene linker at the 3-position of the dihydroindene ring (14) with an ether linker (18) retained the agonist activity, suggesting that the oxygen atom on the fused-ring had little impact on the agonist activity. Aromatic fused-ring compounds with planar structures, such as benzofuran (17) and indole (35), exhibited reduced agonist activities. Nonaromatic ring fused-benzene derivatives bearing an sp³ carbon at the β-position of the propanoic acid moiety appeared to be in a more favorable position of the carboxylic acid relative to compounds bearing an sp² carbon. Finally, introduction of a nitrogen atom into the benzene ring, as with the fused pyridine derivative 32, attenuated the agonist activity compared to the parent compound 14. Generally, a pyridine ring is known as a π–electron-deficient heterocycle, so we speculated that the erosion

of potency on 32 might be attributed to the decreased capability of a π–electron interaction with the GPR40/FFA1 receptor because the π–π interaction between the ligand and the receptor may be important for exerting GPR40/FFA1 activity, as we reported previously.^{22,23}

Next, we screened the GPR40/FFA1 binding affinities in order to identify species differences between humans and rats; this information can be used to examine the *in vivo* insulinotropic effects and glucose-lowering effects during an OGTT using female Wistar fatty rats. Generally, human binding affinities were correlated with human agonist activities as shown in Table 1. However, for the rat receptor, the smaller ring was preferable compared to the larger ring (five-membered ring 14, 18 > six-membered ring 15 > seven-membered ring 19), except for the four-membered ring 25.

Table 1. In Vitro Activities of Fused-Ring Alkanoic Acids



compd	acidic portion	FLIPR	binding		Log <i>D</i> ^c at pH 7.4
		human EC ₅₀ (μM) ^a	human <i>K</i> _i (μM) ^b	rat <i>K</i> _i (μM) ^b	
14		0.033 (0.019–0.057)	0.21	0.52	4.40
15		0.027 (0.016–0.045)	0.059	3.7	4.70
16		0.94 (0.64–1.4)	2.4	>10	5.02
17		4.9 (2.4–10)	>10	>10	4.04
18		0.027 (0.019–0.038)	0.17	1.1	3.88
19		0.070 (0.049–0.10)	0.27	>10	4.05
25		0.069 (0.042–0.11)	1.2	>10	4.12
32		0.57 (0.38–0.86)	>10	>10	3.88
35		ND ^d	>10	>10	3.93
1		0.0077 (0.0051–0.012)	0.032	0.054	4.21

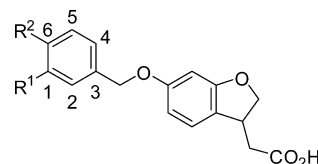
^aEC₅₀ values are averages of *n* = 3 in the presence of 0.1% BSA. EC₅₀ values and 95% confidence intervals of each compound were obtained with Prism 5 software (GraphPad). ^bAll values are averages of *n* = 2 in the presence of 0.2% BSA. ^cLog *D* values were determined at pH 7.4 according to a reported method.³³ ^dNot determined (101% increase of control at 10 μM, 2% increase of control at 1 μM).

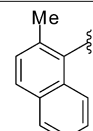
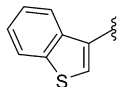
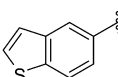
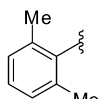
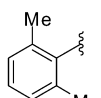
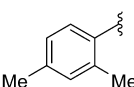
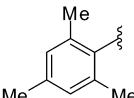
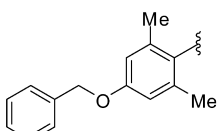
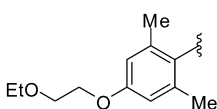
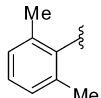
Thus, we identified various nonaromatic ring fused-benzene derivatives with potent GPR40/FFA1 agonist activities and human and rat binding affinities. Among these, the five-membered fused-ring compounds (**14** and **18**) showed potent activities and an acceptable profile regarding species differences. Meanwhile, higher lipophilicity of the compounds might be correlated with undesirable absorption, distribution, metabolism, excretion, and toxicology (ADME-Tox) profiles.³² Accordingly, we selected the (2,3-dihydro-1-benzofuran-3-

yl)acetic acid derivative **18** as a template for further investigation based on its low lipophilicity (see Log *D* value).

Having identified a favorable scaffold that was expected to show a long-lasting PK profile, we then shifted our focus on evaluating the lipophilic portion of the structure (Table 2). In a previous report,²³ we demonstrated that the orthogonal conformation of the biphenyl moiety was important in enhancing agonist activity and reducing the influence of binding to serum albumin. With these observations in mind,

Table 2. In Vitro Activities of (2,3-Dihydro-1-benzofuran-3-yl)acetic Acids



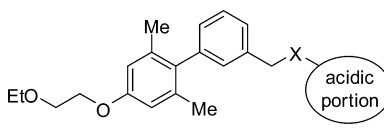
compd	R ¹	R ²	FLIPR	binding		LogD ^c at pH 7.4
			human EC ₅₀ (μM) ^a	human K _i (μM) ^b	rat K _i (μM) ^b	
45		H	0.021 (0.014–0.032)	0.041	0.47	4.33
46		H	0.039 (0.024–0.062)	0.29	>10	3.99
47		H	0.18 (0.11–0.28)	0.57	>10	3.97
48		OMe	0.024 (0.015–0.040)	0.13	1.6	3.31
49		OBn	0.010 (0.0075–0.014)	0.0069	0.17	4.53
50		H	0.029 (0.018–0.045)	0.057	1.6	4.15
51		H	0.033 (0.018–0.061)	0.036	0.13	4.47
52		H	0.028 (0.017–0.047)	0.018	0.10	5.03
53		H	0.028 (0.018–0.043)	0.032	0.20	3.83
18		H	0.027 (0.019–0.038)	0.17	1.1	3.88

^aEC₅₀ values are averages of $n = 3$ in the presence of 0.1% BSA. EC₅₀ values and 95% confidence intervals of each compound were obtained with Prism 5 software (GraphPad). ^bAll values are averages of $n = 2$ in the presence of 0.2% BSA. ^cThe Log D values were determined at pH 7.4 according to a reported method.³³

we first explored bicyclic aromatic rings as an R¹ substituent that would be likely to produce a twisted conformation. The most sterically hindered 2-methyl-1-naphthyl analogue **45** showed comparable agonist activity and higher binding affinities in humans and rats relative to the parent compound **18**. The bioisosteric replacement of the naphthyl group into the 3-benzothienyl group (**46**) showed comparable agonist activity but reduced binding affinities that were likely due to the

absence of an *ortho*-methyl group, and the less hindered 5-benzothiophenyl analogue **47** exhibited lower agonist activity and binding affinities. Next, we evaluated the R² group, the substituent at the 6-position of the central phenyl ring. The 6-methoxy analogue **48** retained activity comparable to the parent compound **18**, and the more sterically bulky 6-benzyloxy analogue **49** displayed significantly improved activity. These results demonstrated the expected results that the steric

Table 3. In Vitro Activities of Fused-Ring Alkanoic Acids



compd	X	acidic portion	FLIPR	binding		Log <i>D</i> ^c at pH 7.4
			human EC ₅₀ (μM) ^a	human <i>K</i> _i (μM) ^b	rat <i>K</i> _i (μM) ^b	
61	O		0.96 (0.64–1.5)	>10	>10	4.11
62	O		0.084 (0.055–0.13)	0.27	>10	4.39
63	O		0.14 (0.091–0.23)	0.28	>10	4.33
64	O		0.51 (0.32–0.80)	2.1	>10	4.67
65	O		0.091(0.055–0.15)	0.39	0.067	3.61
68	O		ND ^d	>10	>10	3.41
73	NH		0.048 (0.031–0.076)	0.043	0.11	3.13
53	O		0.028 (0.018–0.043)	0.032	0.20	3.83

^aEC₅₀ values are averages of *n* = 3 in the presence of 0.1% BSA. EC₅₀ values and 95% confidence intervals of each compound were obtained with Prism 5 software (GraphPad). ^bAll values are averages of *n* = 2 or 3 in the presence of 0.2% BSA. ^cThe Log *D* values were determined at pH 7.4 according to the reported method.³³ ^dNot determined (59% increase of control at 10 μM, 2% increase of control at 1 μM).

bulkiness of the biaryl moiety was important for enhancing the activity of this series. Next, incorporation of a substituent at the 4'-position of the biphenyl group was investigated. Displacement of one methyl group on the 2',6'-dimethyl analogue **18** to the 4'-position (**50**) retained agonist activity and binding affinities in humans and rats. Furthermore, the 2',4',6'-trimethyl analogue **51** also retained potency for the human receptor and showed more potent binding affinities for both human and rat receptors. These results indicated that the introduction of a substituent at the 4'-position was found to be favorable for human and rat binding affinities. Both the 4'-benzyloxy analogue **52** and the 4'-(2-ethoxyethoxy) analogue **53** showed potent agonist activities, suggesting the potential of the incorporation of various substituents, especially a certain level of a polar functionality for modulating drug-like parameters, at the 4'-position of the biphenyl ring.

As described previously, the dihydrobenzofuran derivatives possessed high affinity for the human receptor but reduced affinity for the rat receptor. To examine the influence of the

ring type and the tether on the carboxylic acid moiety, we again explored the acidic portion with the aim of optimally projecting the carboxylic acid moiety toward the acid-binding residue (Table 3). We selected the 4'-(2-ethoxyethoxy)-2',6'-dimethyl-biphenyl group on **53** with a relatively low Log *D* value (3.83) and good PK profile (vide infra) as the lipophilic portion and first screened indane and tetrahydronaphthalene derivatives (**61**–**64**). Unfortunately, all analogues displayed decreased potency, particularly with respect to rat receptor binding affinity. On the other hand, the isobenzofuran analogue **65** retained agonist activity; furthermore, **65** exhibited higher affinity to rat receptors than to human receptors. The oxyindole derivative **68**, which was intended to increase the polarity of the fused-ring moiety (see low Log *D* value), showed decreased potency. This result implied that the carbonyl group of **68** might interrupt the proper interaction with the receptor. Replacement of the linker oxygen of **53** to nitrogen (**73**) minimally affected the agonist activity but decreased the Log *D* value (ca. 0.7). Subsequently, we found that (2,3-dihydro-1-

benzofuran-3-yl)acetic acid was the most effective acidic moiety in this structural series and discovered that the nitrogen linker also appeared to be optimal for potency.

Next, we considered the species differences between human and rat GPR40/FFA1 using homology modeling based on the crystal structure of bovine rhodopsin. The method for modeling and ligand docking was described in a previous paper.²² GPR40/FFA1 is well-conserved between humans and rats; rat GPR40/FFA1 has a 75% identity to human GPR40/FFA1 at the DNA level and an 82% identity to human GPR40/FFA1 at the protein level.² Among the amino acid residues that interact with the ligand in the binding pocket, the only amino acid residue that varies between human and rat might be Leu186 (TMS), which is replaced with Phe in rat GPR40/FFA1. We constructed a rat GPR40/FFA1 model by replacing Leu186 with Phe. Then, we docked the dihydrobenzofuran derivative **18** into this model and superimposed the six-membered analogue **15** and the seven-membered analogue **19** (Figure 4A). In this model, the fused-rings of these compounds were located adjacent to Phe186, indicating that the larger ring caused steric repulsion with the phenyl group of Phe186. Thus, the species differences in the potency between human and rat might result from a decreased affinity due to the substitution of Leu186 in the human GPR40/FFA1 receptor with the sterically bulky Phe in the rat GPR40/FFA1 receptor.

Next, we compared the binding mode of the representative compound **53** with 2-ethoxyethoxy group at the 4'-position of the biphenyl ring and the dihydrobenzofuran lead **18** in the human GPR40/FFA1 receptor (Figure 4B). Compound **53** overlaps well with **18**, and the proposed binding mode of **53** shows several interactions of the {6-[(2',6'-dimethylbiphenyl-3-yl)methoxy]-2,3-dihydro-1-benzofuran-3-yl}acetic acid moiety. The carboxylic acid group interacts with Arg183 (TMS) and Arg258 (TM7), and the benzyl moiety forms a π - π interaction with Trp72 (E-I loop). In addition, 2-ethoxyethoxy group that is characteristic of **53** extends to the space between TM1 and TM7 and might interact with Tyr12 (TM1) and Lys259 (TM7). This information also afforded the opportunity to investigate the effect of the substituent at the 4'-position of the biphenyl ring.

Table 4 shows our data regarding the rat PK profiles for the selected fused-ring alkanolic acids. We initially investigated the relationship between the fused-ring structure and PK profiles (indane **14**, tetrahydronaphthalene **15**, dihydrobenzofuran **18**, and tetrahydrobenzoxepine **19**). Each compound showed superior PK profiles, in particular, a lower clearance and a higher plasma exposure (see $AUC_{po,0-8\text{ h}}$) than phenylpropanoic acid **1** as we had expected. Among these, cyclic ether derivatives (**18** and **19**) exhibited better PK profiles compared to cycloalkane analogues (**14** and **15**). This improvement was likely due to the blocking of the metabolically labile benzylic position on the fused-ring (Figure 5, site A). The most potent 6-benzyloxy analogue **49** showed high clearance, which resulted in decreased plasma exposure (Figure 5, site B), but its bioavailability was still good ($F = 52.4\%$). The rapid clearance of **49** from plasma was probably due to its high tissue distribution consistent with its high lipophilicity (Log D value: 4.53). Introduction of the methyl group into the 4'-position of the distal phenyl group (**51**) decreased the plasma exposure ($AUC_{po,0-8\text{ h}} = 698.7\text{ ng}\cdot\text{h}/\text{mL}$). In contrast, 4'-alkoxy analogues (**52** and **53**), masked at the benzylic position of the distal phenyl ring (Figure 5, site C) with an oxygen atom, showed a good PK profile. In particular,

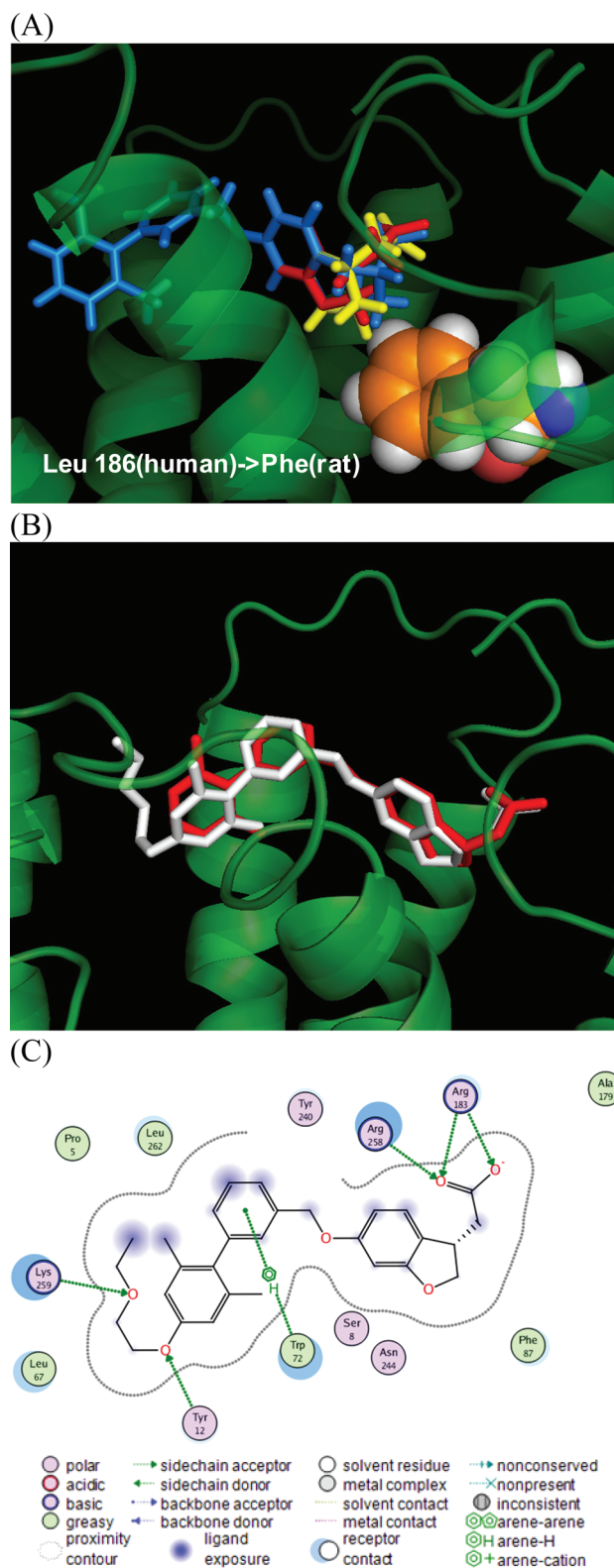


Figure 4. (A) Docking model of GPR40/FFA1 in complex with **15** (yellow), **18** (red), and **19** (blue). (B) Overlay of **18** (red) and **53** (white) in complex with human GPR40/FFA1. (C) Two-dimensional diagram showing the interaction of **53** with human GPR40/FFA1 constructed by MOE.

the 4'-ethoxyethoxy analogue (**53**) exhibited the lowest clearance (211 mL/h/kg) and the highest plasma exposure ($AUC_{po,0-8\text{ h}} = 2837.4\text{ ng}\cdot\text{h}/\text{mL}$) among this series. Analogues

Table 4. PK Profiles for Fused-Ring Alkanoic Acids^a

compd	CL _{total} (mL/h/kg)	C _{max} (ng/mL)	T _{max} (h)	AUC _{po,0-8 h} (ng·h/mL)	F (%)
14	464	285.1	1.67	1701.3	47.8
15	782	220.7	1.33	925.7	56.9
18	296	449.7	2.67	2357.3	69.4
19	293	606.6	1.33	2801.4	68.6
49	1708	84.9	1.00	308.9	52.4
51	625	162.8	2.67	698.7	43.3
52	414	316.9	2.00	1687.8	69.4
53	211	465.4	2.67	2837.4	59.5
65	573	193.1	1.33	871.2	49.2
73	348	439.0	1.67	2230.6	70.2
1	900	86.0	1.50	249.0	21.5

^aRat cassette dosing at 0.1 mg/kg, iv and 1 mg/kg, po. All values are averages of 3 rats. F indicates bioavailability.

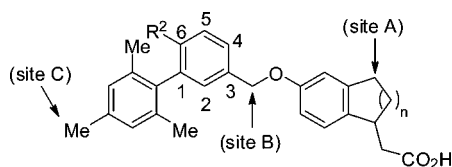


Figure 5. Presumed metabolic sites of fused-ring alkanoic acids.

with the amino linker (73) also showed high exposures and good bioavailabilities that were comparable to the oxygen analogue 53. Overall, the fused-ring alkanoic acids possessed good PK profiles such as low clearance and high plasma exposure, presumably by blocking β -oxidation of the phenyl-

alkanoic acid moiety, indicating that constructing a fused-ring structure would be an efficient strategy for identifying long-acting compounds.

On the basis of its favorable in vitro activity and PK profile, compound 53 was selected and assessed for its ability to improve glucose tolerance during an OGTT in female Wistar fatty rats, which were used as a model developing obesity and obesity-related features such as impaired glucose tolerance, hyperinsulinemia, and hyperlipidemia.³⁴ To evaluate both the intrinsic and durable efficacy of 53, the compound was orally administered 1 and 4 h prior to the glucose challenge (1 g/kg) (these tests were referred as 1H-OGTT and 4H-OGTT, respectively). Single oral dosing of 53 (1, 10 mg/kg) reduced plasma glucose levels (Figure 6A) and augmented insulin secretion (Figure 6C) during 1H-OGTT. The minimum effective dose of the area under the curve of plasma glucose (AUC_{0-120 min}) (Figure 6B) and plasma insulin (AUC_{pre-120 min}) (Figure 6D) was 10 mg/kg. Furthermore, 53 significantly improved glucose tolerance and increased plasma insulin levels during 4H-OGTT at a similar dose as 1H-OGTT (10 mg/kg) (Figure 7A–D). Thus, the dihydrobenzofuran derivative showed durable efficacy due to its desirable PK profile, so this structural series was considered to have a superior profile compared to the phenylpropanoic acid series with high plasma clearance. Additionally, because dihydrobenzofuran derivatives possess higher affinities to the human receptor than to the rat receptor, they are expected to show more potent efficacy in humans. These results encouraged us to focus on a dihydrobenzofuran derivative as a promising lead compound

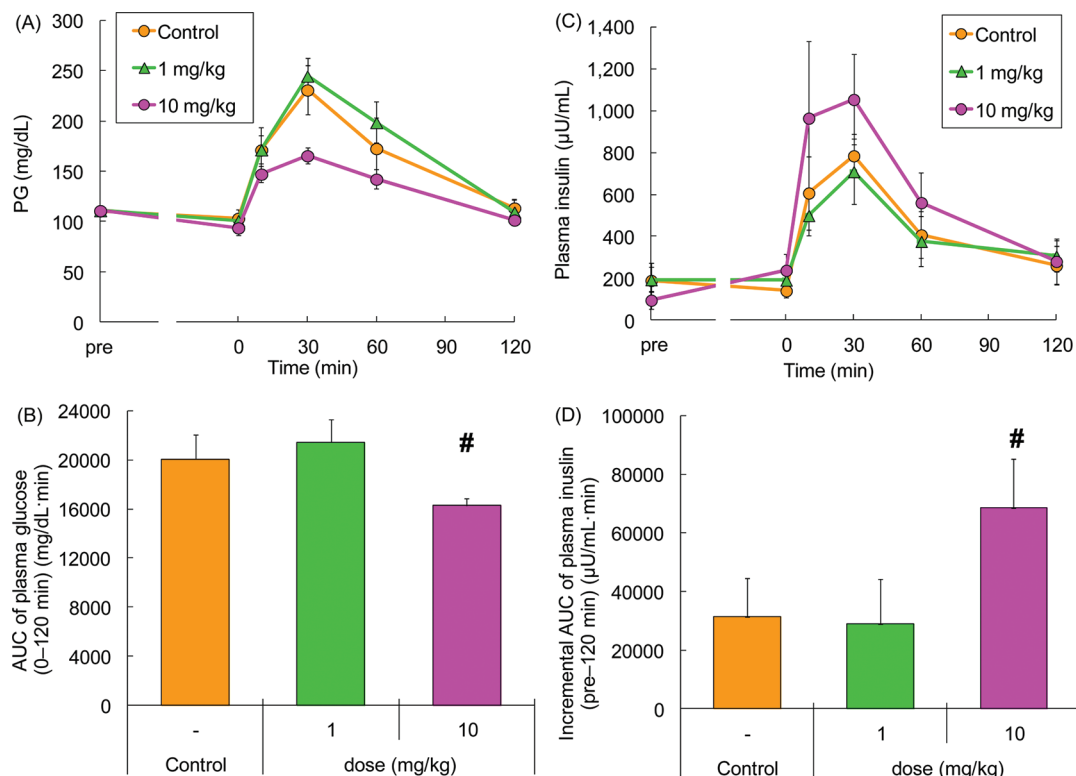


Figure 6. Effects of 53 during an 1H-OGTT in female Wistar fatty rats. (A) and (C) show time-dependent changes of plasma glucose (PG) and plasma insulin levels after single oral doses of 53 (1, 10 mg/kg) followed by 1 g/kg oral glucose challenge, respectively. Data in (B) and (D) represent AUC_{0-120 min} of PG levels and incremental AUC_{0-120 min} of plasma insulin levels shown in (A) and (C), respectively. Values are mean \pm SD ($n = 6$). #: $P \leq 0.025$ compared with control by one-tailed Williams' test.

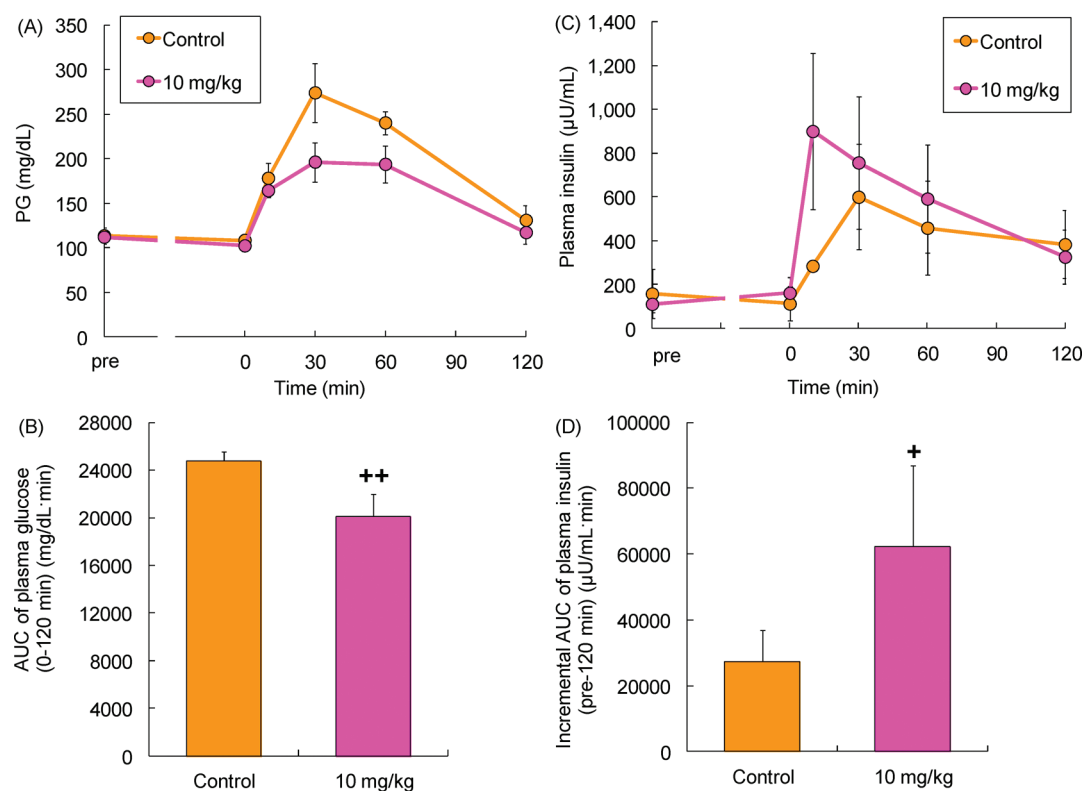


Figure 7. Effects of 53 during a 4H-OGTT in female Wistar fatty rats. (A) and (C) show time-dependent changes of plasma glucose (PG) and plasma insulin levels after single oral doses of 53 (10 mg/kg) followed by 1 g/kg oral glucose challenge, respectively. Data in (B) and (D) represent $AUC_{0-120 \text{ min}}$ of PG levels and incremental $AUC_{0-120 \text{ min}}$ of plasma insulin levels shown in (A) and (C), respectively. Values are mean \pm SD ($n = 5-6$). +, $P \leq 0.05$; ++, $P \leq 0.01$ compared with control by Aspin-Welch test.

to identify new chemical entities with potent, durable, and safe profiles.

CONCLUSION

We identified a series of fused-ring alkanolic acids as potent and orally available GPR40/FFA1 agonists. Cyclization of the phenylpropanoic acid moiety improved the PK profile, especially with respect to clearance and plasma exposure. This effect is consistent with the suppression of metabolic pathways for β -oxidation. Our bioisosteric replacement of the propanoic acid moiety with the fused-ring alkanolic acid moiety provided an efficient strategy for retaining the activity against the target molecule and improving the PK profile. Among this series, (2,3-dihydro-1-benzofuran-3-yl)acetic acid was identified as the best acidic moiety regarding human agonist activity and rat binding affinity, and optimization of its biaryl moiety led to the discovery of 4'-(ethoxyethoxy)-2',6'-dimethylbiphenyl derivative 53 with the lowest clearance and the highest plasma exposure. Compound 53 exhibited a plasma glucose-lowering effect and insulinotropic effect at an oral dose of 10 mg/kg in both 1H-OGTT and 4H-OGTT in female Wistar fatty rats. While 53 presented the concept of a long-acting GPR40 agonist, the effective dose (10 mg/kg) was relatively high in 1H-/4H-OGTTs in female Wistar fatty rats. In addition, the lipophilicity of 53 was still high (Log D value: 3.83). Further optimization to improve potency, physicochemical properties, and ADME profiles suitable for a clinical candidate, resulting in the discovery of TAK-875, will be reported in a forthcoming publication.

EXPERIMENTAL SECTION

Chemistry. Reagents and solvents were obtained from commercial sources and used without further purification. Reaction progress was determined by thin layer chromatography (TLC) analysis on Merck Kieselgel 60 F254 plates or Fuji Silysia NH plates. Chromatographic purification was carried out on silica gel columns (Merck Kieselgel 60, 70–230 mesh or 230–400 mesh, Merck or Chromatorex NH-DM 1020, 100–200 mesh) or on Purif-Pack (SI: 60 μ M or NH: 60 μ M, Fuji Silysia Chemical, Ltd.). Melting points were determined on a BÜCHI B-545 melting point apparatus and were uncorrected. Proton nuclear magnetic resonance (^1H NMR) spectra were recorded on Bruker Ultra Shield-300 (300 MHz) instruments. Chemical shifts are given in parts per million (ppm) with tetramethylsilane as an internal standard. Abbreviations are used as follows: s = singlet, d = doublet, t = triplet, q = quartet, m = multiplet, dd = doublet of doublets, dt = doublet of triplets, td = triplet of doublets, ddd = doublet of doublets of doublets, br = broad. Coupling constants (J values) are given in hertz (Hz). Low-resolution mass spectra (MS) were determined on a Waters liquid chromatography–mass spectrometer system (MS), using a CAPCELL PAK UG-120 ODS (Shiseido Co., Ltd.) column (2.0 mm i.d. \times 50 mm) with aqueous CH_3CN (10–95%) containing 0.05% trifluoroacetic acid (TFA) and an HP-1100 (Agilent Technologies) apparatus for monitoring at 220 nm. All MS experiments were performed using electrospray ionization (ESI) in positive ion mode. Analytical HPLC was performed on a Shimadzu LC-VP instrument, equipped with CAPCELL PAK C18 UG120 S-3 μ m, 2.0 mm \times 50 mm column with a 4 min linear gradient from 90/10 to 5/95 and subsequently with a 1.5 min isocratic elution 5/95 A/B, where A = H_2O –0.1% TFA, B = CH_3CN –0.1% TFA, at a flow rate of 0.5 mL/min, with UV detection at 220 nm, at column temperature of 25 $^\circ\text{C}$, or performed on a Waters Quattro micro API (Agilent HP1100, Gilson215) instrument, equipped with CAPCELL PAK C18 UG120 S-3 μ m, 1.5 mm \times 35 mm column, by gradient elution: 0.00 min (A/B = 100/0), 2.00 min (A/B = 0/100), 3.00 (A/B = 0/100),

3.01 (A/B = 100/0), 3.30 (A/B = 100/0), where A = 2% CH₃CN/H₂O with 5 mM NH₄OAc, B = 95% CH₃CN/H₂O with 5 mM NH₄OAc, at a flow rate of 0.5 mL/min, with UV detection at 220 nm, at column temperature of 40 °C. A part of compounds were assessed by the following method. The analytical HPLC system consisted of Prominence UFLC (Shimadzu Corporation, Japan), L-column2 ODS column (30 mm × 2.1 mm I.D., 2 μm) (Chemicals Evaluation and Research Institute, Japan) at column temperature of 50 °C and nano quantity analyte detector, QT-500 (Quant technologies LLC, MN, USA). The mobile phase A and B are a mixture of distilled water, 50 mmol/L ammonium acetate aqueous solution, and acetonitrile (8:1:1,v/v/v) and a mixture of acetonitrile and 50 mmol/L ammonium acetate aqueous solution (9:1,v/v), respectively. The flow rate maintained 0.5 mL/min. The mixture ratio of mobile phase A and B changed from 95/5 to 5/95 with a 2 min linear gradient and subsequently with a 1 min isocratic elution 5/95. Elemental analyses were carried out by Takeda Analytical Laboratories Limited and were within 0.4% of the theoretical values unless otherwise noted. The purity of compounds was assessed by elemental analysis or analytical HPLC (>95%). Experimental procedures for compounds 14–19 including their intermediates were disclosed in the previous literature (Supporting Information).²¹

4'-Hydroxy-2',6'-dimethylbiphenyl-3-carbaldehyde (44). 4-Bromo-3,5-dimethylphenol (43) 10.3 g, 51.0 mmol) and (3-formylphenyl)boronic acid (7.67 g, 51.2 mmol) were dissolved in a mixture of 1 M sodium carbonate aq (150 mL), EtOH (50 mL), and toluene (150 mL). After argon substitution, tetrakis-(triphenylphosphine)palladium(0) (2.95 g, 2.55 mmol) was added. The reaction mixture was stirred at 80 °C under argon atmosphere for 24 h. The reaction mixture was cooled, and water was added. The mixture was diluted with AcOEt, and the insoluble material was filtered off through Celite. The organic layer of the filtrate was washed with brine, dried over anhydrous magnesium sulfate, and concentrated. The residue was purified by silica gel column chromatography (AcOEt–hexane = 10:90–40:60) to give a solid, which was triturated with hexane–AcOEt to give 44 (9.53 g, 83%) as pale-yellow crystals. ¹H NMR (CDCl₃) δ 1.97 (s, 6H), 4.69 (s, 1H), 6.62 (s, 2H), 7.42 (dt, J = 7.7, 1.4 Hz, 1H), 7.59 (t, J = 7.6 Hz, 1H), 7.66 (t, J = 1.7 Hz, 1H), 7.86 (dt, J = 7.6, 1.5 Hz, 1H), 10.05 (s, 1H). MS *m/z* 227 (M + H)⁺.

[4'-(2-Ethoxyethoxy)-2',6'-dimethylbiphenyl-3-yl]methanol (42i). Step 1: A mixture of 44 (8.52 g, 37.7 mmol), 2-chloroethyl ethyl ether (6.15 g, 56.6 mmol), K₂CO₃ (6.25 g, 45.2 mmol), and KI (1.25 g, 7.54 mmol) in DMF (40 mL) was stirred under nitrogen atmosphere at 80 °C for 18 h. After evaporation of the solvent, the residue was partitioned between water and AcOEt. The extract was washed with brine, dried over anhydrous MgSO₄, and concentrated. The residue was purified by silica gel column chromatography (AcOEt–hexane = 5:95–25:75) to give 4'-(2-ethoxyethoxy)-2',6'-dimethylbiphenyl-3-carbaldehyde (10.0 g, 89%) as a colorless oil. ¹H NMR (CDCl₃) δ 1.26 (t, J = 7.0 Hz, 3H), 1.99 (s, 6H), 3.62 (q, J = 7.0 Hz, 2H), 3.81 (t, J = 4.9 Hz, 2H), 4.15 (t, J = 4.9 Hz, 2H), 6.71 (s, 2H), 7.42 (dt, J = 7.5, 1.5 Hz, 1H), 7.58 (t, J = 7.5 Hz, 1H), 7.66 (t, J = 1.5 Hz, 1H), 7.86 (dt, J = 7.5, 1.5 Hz, 1H), 10.05 (s, 1H). MS *m/z* 299 (M + H)⁺. Step 2: To a solution of the obtained oil (4.21 g, 14.1 mmol) in MeOH (15 mL) and THF (30 mL) was added portionwise NaBH₄ (0.533 g, 14.1 mmol) at 0 °C, and the mixture was stirred under nitrogen atmosphere at 0 °C for 2 h. The mixture was quenched with water and 1 M HCl aqueous solution and extracted with AcOEt. The extract was washed with brine, dried over anhydrous Na₂SO₄, and concentrated. The residue was purified by silica gel column chromatography (AcOEt–hexane = 20:80–60:40) to give a solid. Recrystallization from hexane–AcOEt gave 42i (3.37 g, 79%) as colorless crystals. ¹H NMR (CDCl₃) δ 1.25 (t, J = 7.1 Hz, 3H), 1.66 (t, J = 5.9 Hz, 1H), 2.00 (s, 6H), 3.62 (q, J = 7.1 Hz, 2H), 3.80 (t, J = 5.1 Hz, 2H), 4.14 (t, J = 5.1 Hz, 2H), 4.73 (d, J = 5.9 Hz, 2H), 6.69 (s, 2H), 7.06 (d, J = 7.3 Hz, 1H), 7.12 (s, 1H), 7.33 (d, J = 7.3 Hz, 1H), 7.40 (t, J = 7.3 Hz, 1H). MS *m/z* 301 (M + H)⁺.

{6-[4'-(2-Ethoxyethoxy)-2',6'-dimethylbiphenyl-3-yl]methoxy}-2,3-dihydro-1-benzofuran-3-yl}acetic Acid (53). Step 1: To a mixture of 7e (0.250 g, 1.20 mmol), 42h (0.330 g, 1.10 mmol),

and tributylphosphine (0.448 mL, 1.80 mmol) in toluene (20 mL) was added portionwise 1,1'-(azodicarbonyl)dipiperidine (0.454 g, 1.80 mmol) at 0 °C, and the mixture was stirred at room temperature under nitrogen atmosphere for 15 h. Hexane (10 mL) was added, and the insoluble material was removed by filtration. The filtrate was concentrated, and the residue was purified by silica gel column chromatography (AcOEt–hexane = 5:95–30:70) to give methyl {6-[4'-(2-ethoxyethoxy)-2',6'-dimethylbiphenyl-3-yl]methoxy}-2,3-dihydro-1-benzofuran-3-yl}acetate (0.481 g, 89%) as a colorless oil. ¹H NMR (CDCl₃) δ 1.25 (t, J = 7.1 Hz, 3H), 1.98 (s, 6H), 2.55 (dd, J = 16.5, 9.2 Hz, 1H), 2.75 (dd, J = 16.5, 5.4 Hz, 1H), 3.62 (q, J = 7.1 Hz, 2H), 3.71 (s, 3H), 3.75–3.85 (m, 3H), 4.14 (t, J = 5.1 Hz, 2H), 4.26 (dd, J = 9.2, 6.0 Hz, 1H), 4.75 (t, J = 9.2 Hz, 1H), 5.05 (s, 2H), 6.45–6.50 (m, 2H), 6.68 (s, 2H), 7.01 (d, J = 8.1 Hz, 1H), 7.08 (dt, J = 7.0, 1.6 Hz, 1H), 7.16 (s, 1H), 7.35–7.44 (m, 2H). MS *m/z* 491 (M + H)⁺. Step 2: To a solution of methyl {6-[4'-(2-ethoxyethoxy)-2',6'-dimethylbiphenyl-3-yl]methoxy}-2,3-dihydro-1-benzofuran-3-yl}acetate (1.96 g, 4.00 mmol) in MeOH (20 mL) and THF (20 mL) was added 2 M NaOH aqueous solution (6 mL), and the mixture was stirred at room temperature for 3 days. The mixture was diluted with water, acidified with 10% citric acid aqueous solution, and extracted with AcOEt. The organic layer was washed with brine, dried over MgSO₄, and concentrated. The residue was purified by silica gel column chromatography (AcOEt–hexane = 20:80–80:20) and crystallized from heptane–AcOEt to give 53 (1.12 g, 59%) as colorless prisms; mp 72 °C. ¹H NMR (CDCl₃) δ 1.25 (t, J = 7.1 Hz, 3H), 1.98 (s, 6H), 2.61 (dd, J = 16.8, 9.2 Hz, 1H), 2.80 (dd, J = 16.8, 5.4 Hz, 1H), 3.62 (q, J = 7.1 Hz, 2H), 3.75–3.85 (m, 3H), 4.14 (t, J = 5.0 Hz, 2H), 4.28 (dd, J = 9.2, 6.0 Hz, 1H), 4.75 (t, J = 9.2 Hz, 1H), 5.05 (s, 2H), 6.45–6.51 (m, 2H), 6.68 (s, 2H), 7.03–7.10 (m, 2H), 7.16 (s, 1H), 7.34–7.44 (m, 2H). MS *m/z* 477 (M + H)⁺. HPLC purity (220 nm) 100%. Anal. Calcd for C₂₉H₃₂O₆: C, 73.09; H, 6.77. Found: C, 73.06; H, 6.73.

Ca Influx Activity of CHO Cells Expressing Human GPR40/FFA1 (FLIPR Assay). CHO dhfr cells stably expressing human GPR40/FFA1 (accession no. NM_005303) were plated and incubated overnight in 5% CO₂ at 37 °C. Then, cells were incubated in loading buffer (recording medium containing 2.5 μg/mL fluorescent calcium indicator Fluo 4-AM (Molecular Devices), 2.5 mmol/L probenecid (Dojindo), and 0.1% fatty acid-free BSA (Sigma)) for 60 min at 37 °C. Various concentrations of test compounds or γ-linolenic acid (Sigma) were added into the cells and increase of the intracellular Ca²⁺ concentration after addition were monitored by FLIPR Tetra system (Molecular Devices) for 90 s. The agonistic activities of test compounds and γ-linolenic acid on human GPR40/FFA1 were expressed as [(A – B)/(C – B)] × 100 (increase of the intracellular Ca²⁺ concentration (A) in test compounds-treated cells, (B) in vehicle-treated cells, and (C) in 10 μM γ-linolenic acid-treated cells). EC₅₀ values and 95% confidence intervals of each compound were obtained with Prism 5 software (GraphPad).

Preparation of CHO Membrane for GPR40/FFA1 Receptor Binding Assay. Cell lines stably expressing human GPR40/FFA1 and rat GPR40/FFA1 were used for the experiments. Each cell was cultured in Minimum Essential Medium Alpha (MEM-Alpha, Invitrogen) supplemented with 10% dialyzed Fetal-Bovine-Serum (dialyzed FBS, Thermo Trace Ltd.), 100 unit/mL penicillin, and 100 unit/mL streptomycin in 5% CO₂/95% air atmosphere at 37 °C. Cells were harvested at confluence in Dulbecco's Phosphate-Buffered-Saline (D-PBS, Invitrogen) containing 1 mM EDTA and centrifuged. Cells were homogenized in ice-cold membrane preparation buffer (50 mM Tris-HCl (pH 7.5), 5 mM EDTA, 0.5 mM PMSF (Wako), 20 μg/mL leupeptin, 0.1 μg/mL pepstatin A, 100 μg/mL Phosphoramidon, Peptide Institute, Inc.) and centrifuged (700g, 10 min, 4 °C). The supernatant was filtered through 40 μm Cell Strainer (BD Falcon) and ultracentrifuged (100000g, 1 h, 4 °C) with Optima L-100 XP Ultracentrifuge (Beckman Coulter). The precipitation was suspended in the same buffer, and the protein concentration was determined with the BCA Protein assay reagent (Pierce) following membrane solubilization with 0.1% SDS and 0.1 M NaOH aqueous solution.

The membrane suspension was stored at $-80\text{ }^{\circ}\text{C}$ until receptor binding assay.

GPR40/FFA1 Receptor Binding Assay. The frozen cell membranes were resuspended in ice-cold assay buffer (25 mmol/L Tris-HCl (pH7.5), 5 mmol/L EDTA, 0.5 mmol/L PMSF, 20 $\mu\text{g}/\text{mL}$ leupeptin, 0.1 $\mu\text{g}/\text{mL}$ pepstatin A, 0.05% CHAPS (Wako), and 0.2% fatty-acid-free BSA (Sigma)) and used for receptor binding assay. To determine the K_d values of 3-[4-(2',6'-dimethyl-6-[(4-[^3H]-phenylmethoxy]biphenyl-3-yl)methoxy)phenyl] propanoic acid (Amersham Biosciences) for human and rat GPR40/FFA1, binding assays were performed in the presence of various concentrations of the labeled ligand. After incubation at room temperature for 90 min, the membranes were harvested GF/C filter plates (MILLIPORE) and washed with ice-cold 50 mmol/L Tris-HCl (pH7.5) using FilterMate Harvester (PerkinElmer). The membrane-associated radioactivities were counted using TopCount liquid scintillation counter (PerkinElmer). Nonspecific binding was defined as binding in the presence of 10 $\mu\text{mol}/\text{L}$ of the unlabeled ligand. To determine the binding affinities of test compounds to human and rat GPR40/FFA1, binding assays were performed in the presence of both various concentrations of test compounds and 2 nmol/L or 6 nmol/L of the labeled ligand. The 50% inhibitory concentrations (IC_{50} values) of test compounds for the labeled ligand were calculated using nonlinear regression analysis in GraphPad Prism 3.0 (GraphPad Software). K_i values were converted as $K_i = \text{IC}_{50}/\{1 + (\text{the concentration of the labeled ligand})/\text{K}_d\}$.

Molecular Modeling. A homology model of GPR40/FFA1 was constructed using the crystal structure of bovine rhodopsin (PDB code 1GZM),³⁵ which was obtained from the RCSB Protein Data Bank, as a structural template. An alignment of the amino acid sequences between human/rat GPR40/FFA1 and rhodopsin was created using ClustalX (version 2.0.11)³⁶ and manually revised. Procedures of homology modeling were performed in MOE (version 2008.10).³⁷ The CL2 loop on the extra cellular domain was excluded except Cys170 forming disulfide bond due to the difficulty of estimation. In the previous step, compound **18** was docked into the obtained receptor model using the program GOLD (version 4.1).³⁸ Then, the resultant docking modes with receptor models, replacing compound **18** with **15**, **19**, or **53**, were subjected energy minimization with MOE after connecting each residual substituent. In the energy minimization process, the MMFF94s force field was used and the dielectric constant was set to $2r$, where r is the distance between two interacting atoms.

Pharmacokinetic Analysis in Rat Cassette Dosing. Test compounds were administered as a cassette dosing to nonfasted rats. After oral and intravenous administration, blood samples were collected. The blood samples were centrifuged to obtain the plasma fraction. The plasma samples were deproteinized with acetonitrile containing an internal standard. After centrifugation, the supernatant was diluted and centrifuged again. The compound concentrations in the supernatant were measured by LC/MS/MS.

Oral Glucose Tolerance Test (OGTT). The care and use of the animals and the experimental protocols used in this research were approved by the Experimental Animal Care and Use Committee of Takeda Pharmaceutical Company Limited. Female Wistar fatty (WF) rats were obtained from Takeda Rabics, Ltd. (Hikari, Japan). They were fed a commercial diet CE-2 (Clea Japan Co.) and tap water ad libitum. Female WF rats (17–19 weeks old) were fasted overnight and orally given vehicle (0.5% methylcellulose) or compounds. All animals were received an oral glucose load (1 g/kg) 1 or 4 h after drug administration. Blood samples were collected from tail vein before drug administration (pre), and just before glucose load (time 0), and 10, 30, 60, and 120 min after glucose load. Plasma glucose and plasma insulin levels were measured by Autoanalyzer 7080 (Hitachi, Japan) and radioimmunoassay (Millipore, USA), respectively. In the dose-dependent study, statistical significances versus vehicle control were assessed by one-tailed Williams test. Differences between two groups were analyzed by Aspin–Welch test.

■ ASSOCIATED CONTENT

■ Supporting Information

Synthetic procedures and spectroscopic data of final compounds and intermediates not described in the manuscript. This material is available free of charge via the Internet at <http://pubs.acs.org>.

■ AUTHOR INFORMATION

Corresponding Author

*Phone: +81-466-32-1279. Fax: +81-466-29-4536. E-mail: Negoro_Nobuyuki@takeda.co.jp.

Notes

The authors declare no competing financial interest.

■ ACKNOWLEDGMENTS

We thank Dr. Nozomu Sakai, Satoshi Mikami, Nobuyuki Amano, and Junichi Sakamoto for helpful discussions and Dr. Tsuyoshi Maekawa for proofreading this manuscript.

■ ABBREVIATIONS USED

GPR40/FFA1, G protein-coupled receptor 40/free fatty acid receptor 1; PK, pharmacokinetic; OGTT, oral glucose tolerance test; GSIS, glucose-stimulated insulin secretion; FFA, free fatty acid; DPP-4, dipeptidyl peptidase-4; GLP-1, glucagon-like peptide-1; rt, room temperature; aq, aqueous; FLIPR, fluorometric imaging plate reader; CHO, Chinese hamster ovary; BSA, bovine serum albumin; ADME-Tox, absorption, distribution, metabolism, excretion, and toxicology; CL, plasma clearance; C_{max} , maximum plasma concentration; AUC, area under curve; T_{max} , time of maximum plasma concentration; AUC, area under curve; PG, plasma glucose

■ REFERENCES

- (1) Itoh, Y.; Kawamata, Y.; Harada, M.; Kobayashi, M.; Fujii, R.; Fukusumi, S.; Ogi, K.; Hosoya, M.; Tanaka, Y.; Uejima, H.; Tanaka, H.; Maruyama, M.; Satoh, R.; Okubo, S.; Kizawa, H.; Komatsu, H.; Matsumura, F.; Noguchi, Y.; Shinohara, T.; Hinuma, S.; Fujisawa, Y.; Fujino, M. Free fatty acids regulate insulin secretion from pancreatic β cells through GPR40. *Nature* **2003**, *422*, 173–176.
- (2) Briscoe, C. P.; Tadayyon, M.; Andrews, J. L.; Benson, W. G.; Chambers, J. K.; Eilert, M. M.; Ellis, C.; Elshourbagy, N. A.; Goetz, A. S.; Minnick, D. T.; Murdock, P. R.; Sauls, H. R.; Shabon, U.; Spinage, L. D.; Strum, J. C.; Szekeres, P. G.; Tan, K. B.; Way, J. M.; Ignar, D. M.; Wilson, S.; Muir, A. I. The orphan G protein-coupled receptor GPR40 is activated by medium and long chain fatty acids. *J. Biol. Chem.* **2003**, *278*, 11303–11311.
- (3) Kotarsky, K.; Nilsson, N. E.; Flodgren, E.; Owman, C.; Olde, B. A human cell surface receptor activated by free fatty acids and thiazolidinedione drugs. *Biochem. Biophys. Res. Commun.* **2003**, *301*, 406–410.
- (4) Shapiro, H.; Shachar, S.; Sekler, I.; Hershinkel, M.; Walker, M. D. Role of GPR40 in fatty acid action on the β cell line INS-1E. *Biochem. Biophys. Res. Commun.* **2005**, *335*, 97–104.
- (5) Fujiwara, K.; Maekawa, F.; Yada, T. Oleic acid interacts with GPR40 to induce Ca^{2+} signaling in rat islet β -cells: mediation by PLC and L-type Ca^{2+} channel and link to insulin release. *Am. J. Physiol. Endocrinol. Metab.* **2005**, *289*, E670–E677.
- (6) Gravena, C.; Mathias, P. C.; Ashcroft, S. J. H. Acute effects of fatty acids on insulin secretion from rat and human islets of Langerhans. *J. Endocrinol.* **2002**, *173*, 73–80.
- (7) Poitout, V.; Robertson, R. P. Minireview: Secondary β -cell failure in type 2 diabetes—a convergence of glucotoxicity and lipotoxicity. *Endocrinology* **2002**, *143*, 339–342.
- (8) Robertson, R. P.; Zhang, H. J.; Pyzdrowski, K. L.; Walseth, T. F. Preservation of insulin mRNA levels and insulin secretion in HIT cells

by avoidance of chronic exposure to high glucose concentrations. *J. Clin. Invest.* **1992**, *90*, 320–325.

(9) Boden, G. Obesity, insulin resistance and free fatty acids. *Curr. Opin. Endocrinol. Diabetes Obes.* **2011**, *18*, 139–143.

(10) Rendell, M. The role of sulphonylureas in the management of type 2 diabetes mellitus. *Drugs* **2004**, *64*, 1339–1358.

(11) Doyle, M. E.; Egan, J. M. Pharmacological agents that directly modulate insulin secretion. *Pharmacol. Rev.* **2003**, *55*, 105–131.

(12) Maedler, K.; Carr, R. D.; Bosco, D.; Zuellig, R. A.; Berney, T.; Donath, M. Y. Sulfonylurea induced β -cell apoptosis in cultured human islets. *J. Clin. Endocrinol. Metab.* **2005**, *90*, 501–506.

(13) Del Guerra, S.; Marselli, L.; Lupi, R.; Boggi, U.; Mosca, F.; Benzi, L.; Del Prato, S.; Marchetti, P. Effects of prolonged in vitro exposure to sulphonylureas on the function and survival of human islets. *J. Diabetes Complications* **2005**, *19*, 60–64.

(14) For recent reviews, see: Bharate, S. B.; Nemmani, K. V.S.; Vishwakarma, R. A. Progress in the discovery and development of small-molecule modulators of G-protein-coupled receptor 40 (GPR40/FFA1/FFAR1): an emerging target for type 2 diabetes. *Expert Opin. Ther. Pat.* **2009**, *19*, 237–264.

(15) Garrido, D. M.; Corbett, D. F.; Dwornik, K. A.; Goetz, A. S.; Littleton, T. R.; McKeown, S. C.; Mills, W. Y.; Smalley, T. L.; Briscoe, C. P.; Peat, A. J. Synthesis and activity of small molecule GPR40 agonists. *Bioorg. Med. Chem. Lett.* **2006**, *16*, 1840–1845.

(16) Zhou, C. Y.; Tang, C.; Chang, E.; Ge, M.; Lin, S. N.; Cline, E.; Tan, C. P.; Feng, Y.; Zhou, Y. P.; Eiermann, G. J.; Petrov, A.; Salituro, G.; Meinke, P.; Mosley, R.; Akiyama, T. E.; Einstein, M.; Kumar, S.; Berger, J.; Howard, A. D.; Thornberry, N.; Mills, S. G.; Yang, L. H. Discovery of 5-aryloxy-2,4-thiazolidinediones as potent GPR40 agonists. *Bioorg. Med. Chem. Lett.* **2010**, *20*, 1298–1301.

(17) Song, F. B.; Lu, S. F.; Gunnet, J.; Xu, J. Z.; Wines, P.; Proost, J.; Liang, Y.; Baumann, C.; Lenhard, J.; Murray, W. V.; Demarest, K. T.; Kuo, G. H. Synthesis and biological evaluation of 3-aryl-3-(4-phenoxy)-propionic acid as a novel series of G protein-coupled receptor 40 agonists. *J. Med. Chem.* **2007**, *50*, 2807–2817.

(18) Morrison, H.; Jona, J.; Walker, S. D.; Woo, J. C. S.; Li, L.; Fang, J. Development of a suitable salt form for a GPR40 receptor agonist. *Org. Process Res. Dev.* **2011**, *15*, 104–111.

(19) Christiansen, E.; Due-Hansen, M. E.; Urban, C.; Merten, N.; Pfeleiderer, M.; Karlsen, K. K.; Rasmussen, S. S.; Steensgaard, M.; Hamacher, A.; Schmidt, J.; Drewke, C.; Petersen, R. K.; Kristiansen, K.; Ullrich, S.; Kostenis, E.; Kassack, M. U.; Ulven, T. Structure–activity study of dihydrocinnamic acids and discovery of the potent FFA1 (GPR40) agonist TUG-469. *ACS Med. Chem. Lett.* **2010**, *1*, 345–349.

(20) Christiansen, E.; Urban, C.; Merten, N.; Liebscher, K.; Karlsen, K. K.; Hamacher, A.; Spinrath, A.; Bond, A. D.; Drewke, C.; Ullrich, S.; Kassack, M. U.; Kostenis, E.; Ulven, T. Discovery of potent and selective agonists for the free fatty acid receptor 1 (FFA1)/GPR40, a potential target for the treatment of type II diabetes. *J. Med. Chem.* **2008**, *51*, 7061–7064.

(21) Christiansen, E.; Urban, C.; Grundmann, M.; Due-Hansen, M. E.; Hagesaether, E.; Schmidt, J.; Pardo, L.; Ullrich, S.; Kostenis, E.; Kassack, M.; Ulven, T. Identification of a Potent and Selective Free Fatty Acid Receptor 1 (FFA1/GPR40) Agonist with Favorable Physicochemical and In Vitro ADME Properties. *J. Med. Chem.* **2011**, *54*, 6691–6703.

(22) Negoro, N.; Sasaki, S.; Mikami, S.; Ito, M.; Suzuki, M.; Tsujihata, Y.; Ito, R.; Harada, A.; Takeuchi, K.; Suzuki, N.; Miyazaki, J.; Santou, T.; Odani, T.; Kanzaki, N.; Funami, M.; Tanaka, T.; Kogame, A.; Matsunaga, S.; Yasuma, T.; Momose, Y. Discovery of TAK-875: a potent, selective, and orally bioavailable GPR40 agonist. *ACS Med. Chem. Lett.* **2010**, *1*, 290–294.

(23) Sasaki, S.; Kitamura, S.; Negoro, N.; Suzuki, M.; Tsujihata, Y.; Suzuki, N.; Santou, T.; Kanzaki, N.; Harada, M.; Tanaka, Y.; Kobayashi, M.; Tada, N.; Funami, M.; Tanaka, T.; Yamamoto, Y.; Fukatsu, K.; Yasuma, T.; Momose, Y. Design, synthesis, and biological activity of potent and orally available G protein-coupled receptor 40 agonists. *J. Med. Chem.* **2011**, *54*, 1365–1378.

(24) Node, M.; Kumar, K.; Nishide, K.; Ohsugi, S.; Miyamoto, T. Odorless substitutes for foul-smelling thiols: syntheses and applications. *Tetrahedron Lett.* **2001**, *42*, 9207–9210.

(25) Conconi, M. T.; Guiotto, A.; Manzini, P.; Chilin, A.; Bassani, V.; Parnigotto, P. P. 4-Hydroxymethyltetrahydro- and 4-hydroxymethylbenzopsoralen: synthesis and biological activity. *Farmaco* **1995**, *50*, 125–130.

(26) Fall, Y.; Santana, L.; Teijeira, M.; Uriarte, E. A convenient synthesis of benzofuran-3-acetic acids. *Heterocycles* **1995**, *41*, 647–650.

(27) Kametani, T.; Nemoto, H.; Ishikawa, H.; Shiroyama, K.; Fukumoto, K. A formal regio- and stereoselective total synthesis of estrone. A convenient synthesis of D-homoestrone. *J. Am. Chem. Soc.* **1976**, *98*, 3378–890.

(28) Nishide, K.; Node, M. Development of odorless sulfur reagents and their applications. *J. Syn. Org. Chem. Jpn.* **2004**, *62*, 895–910.

(29) Gao, Y.; Zhang, Q.; Xu, J. A convenient and effective method for synthesizing β -amino- α,β -unsaturated esters and ketones. *Synth. Commun.* **2004**, *34*, 909–916.

(30) Anghelide, N.; Draghici, C.; Raileanu, D. New dienamino esters and their cyclization to α -pyridones of nicotinic acid. *Tetrahedron* **1974**, *30*, 623–632.

(31) Fukuyama, T.; Jow, C.-K.; Cheung, M. 2- and 4-Nitrobenzenesulfonamides: exceptionally versatile means for preparation of secondary amines and protection of amines. *Tetrahedron Lett.* **1995**, *36*, 6373–6374.

(32) Waring, M. J. Lipophilicity in drug discovery. *Expert Opin. Drug Discovery* **2010**, *5*, 235–248.

(33) Yamagami, C.; Ogura, T.; Takao, N. Hydrophobicity parameters determined by reverse-phase liquid chromatography I. Relationship between capacity factors and octanol–water partition coefficients for monosubstituted pyrazines and the related pyridines. *J. Chromatogr.* **1990**, *514*, 123–136.

(34) Ikeda, H.; Shino, A.; Matsuo, T.; Iwatsuka, H.; Suzuoki, Z. A new genetically obese-hyperglycemic rat (Wistar fatty). *Diabetes* **1981**, *30*, 1045–1050.

(35) Li, J.; Edwards, P. C.; Burghammer, M.; Villa, C.; Schertler, G. F. X. Structure of bovine rhodopsin in a trigonal crystal form. *J. Mol. Biol.* **2004**, *343*, 1409–1438.

(36) Larkin, M. A.; Blackshields, G.; Brown, N. P.; Chenna, R.; McGettigan, P. A.; McWilliam, H.; Valentin, F.; Wallace, I. M.; Wilm, A.; Lopez, R.; Thompson, J. D.; Gibson, T. J.; Higgins, D. G. Clustal W and Clustal X version 2.0. *Bioinformatics* **2007**, *23*, 2947–2948.

(37) *Chemical Computing Group Inc.*; Chemical Computing Group Inc., 1010 Sherbrooke Street W, Suite 910 Montreal, Quebec, Canada H3A 2R7; www.chemcomp.com.

(38) *CCDC, Business & Administration*; CCDC, Business & Administration, Cambridge Crystallographic Data Centre, 12 Union Road, Cambridge CB2 1EZ, U.K.; http://www.ccdc.cam.ac.uk.